Acta Mech 230, 1907–1917 (2019)
https://doi.org/10.1007/s00707-019-2375-8

ORIGINAL PAPER

Dalia Čalnerytė · Vidmantas Rimavičius · Rimantas Barauskas

Finite element analysis of resonant properties of silicon nanowires

Received: 23 October 2018 / Revised: 14 January 2019 / Published online: 14 February 2019
© Springer-Verlag GmbH Austria, part of Springer Nature 2019

Abstract This paper presents a 3D nanostructure modal vibration analysis by using finite element models. The modal frequencies and corresponding modal shapes of silicon nanowires of various thickness against length ratios are determined by solving a linear structural eigenvalue problem for the 3D solid finite element model, where surface stress effects are taken into account by using the stress stiffness matrix. The cases of fixed/fixed and fixed/free boundary conditions at the nanowire ends are investigated. The results obtained by 3D solid models and models based on the beam bending theory have been compared with each other, as well as with the results obtained elsewhere in the literature computationally and experimentally. It has been shown that the effects caused by surface stresses are insignificant for wires with length-to-width ratio less than 10.

1 Introduction

The computer simulation of the physical behavior of materials and structures has long been an integral part of the development and design of new products in structural engineering, mechanics, mechatronics, and many other technical fields. Nanoscale structures modeling brings new challenges compared to models formulated for macroscale objects. As an example, the research on cells mobility in a biological field has been investigated in [1], where molecular dynamics modeling has been used for nanomechanical behavior in order to find an approximation of the elastic constants of the cell. Modeling molecular dynamics can also be a useful tool for investigating the mechanical behavior of biological nanomaterials. Another field of application are engines with moving parts, which often have limited construction and service life due to friction and wear. The development of miniature devices, such as microelectromechanical systems and nanometric devices, has increased interest in atomic scale friction, which is very different from macrofriction. An overview of computational studies of nanoscale friction and lubrication calculations, along with the calculation methods used in these studies, is presented in [2].

Recently, the interest in nanotechnology has increased rapidly because of its application in nanoelectronics and other fields [3,4]. The physical behavior of macro- and microscale models can be described by using the principles of classical mechanics of materials, where the surface energy is usually not taken into account [5].

D. Čalnerytė (✉) · V. Rimavičius · R. Barauskas
Department of Applied Informatics, Faculty of Informatics, Kaunas University of Technology, Studentu St. 50-407, 51368 Kaunas, Lithuania
E-mail: dalia.calneryte@ktu.lt

V. Rimavičius
E-mail: vidmantas.rimavicius@ktu.lt

R. Barauskas
E-mail: rimantas.barauskas@ktu.lt

However, in nanoscale models, surface strain and stress may influence the overall stiffness of the body significantly [6]. This factor is important due to the much larger value of surface area against bulk volume ratio of nanoscale models. Different approaches such as molecular dynamics [7,8], analytical and numerical vibration analysis based on the known beam theories with the incorporated surface effects [9–12], and models based on the finite element method [13–15] have been used in order to take into account the decrease in the structural stiffness due to surface stress. However, the approaches based on the classic beam theories are appropriate only for beams with simple cross section. A wide review on the bending, buckling, and vibrational analysis of nanoscale beams is provided in [16] with the section covering the researches on surface effects. In [9], the 3D finite element (FE) model was mentioned as a possible alternative for the analytical Timoshenko beam model. The surface layer was represented by a single layer of 3D solid elements, which made the accuracy of the results highly dependent on the mesh refinement. Moreover, the 3D model was not described in sufficient detail. In [17], the nanoscale elastic body was modeled as a conventional linearly elastic FE structure coated by the prestressed membrane elements. It has been demonstrated that the stresses acting on the boundary surfaces can have significant effects on the modal properties of the nanoscale models [18,19]. Also simplified representations have been extensively used, where the nanoscale effects have been taken into account by introducing the values of equivalent Young's modulus of the nanostructure obtained by comparing certain simulation results against the experimentally obtained values [20–24]. However, this could not be regarded as a robust approach, because the value of the equivalent Young's modulus is often dependent on the size of the structure, as well as on the investigated mode. For a silicon nanowire, when the diameter of the nanowire is less than 100 nm, Young's modulus decreases with decreasing diameter [20,25].

In this paper, we demonstrate that the robust and theoretically well-explicable results are obtained by applying the two-step computational procedure. In our approach, we use the combination of 3D and membrane elements to represent the influence of the surface stresses. This enables to avoid the excessive refinement of the FE domain near the surface, as well as to employ the surface layer characteristics in a more generalized form. Simultaneously, the full set of features of 3D solid model is retained for the representation of the modes. In this way, the analysis is applicable to all volumetric modes of the body rather than being limited to pure longitudinal, flexural, and torsional vibrations of beams. First, the small displacement static equilibrium problem is solved where the load is formulated as initial surface stresses placed on the external faces of the 3D solid elements of the structure with respect to the additional membrane elements with negative stiffness. The obtained stresses of the solid elements are employed to form the stress stiffness matrix of the structure. The structural stress stiffness matrix is used in combination with the conventional stiffness matrix for obtaining the vibration modes via the linear eigenproblem solution. In this way, different types of modes were obtained, and the necessary modal frequency corrections compared with conventional linear models were estimated. The proposed computational procedure is based on the one provided in [20] by adding the terms of the geometrical stiffness matrix for the solid elements in the eigenvalue problem. This enables to take into account the internal stress state of the structure in the vibrational analysis. Moreover, the 2D elements on the surface of the structure enable to prescribe the desirable properties which are necessary to capture the behavior of the surface layer. In addition, in contrast to molecular dynamics, no additional degrees of freedom are generated in the finite element model of the surface layer using this approach which results in effective computational resources. As an alternative approach, the axially prestressed bent beam elements structure analysis may be used to estimate how much the calculated modal frequency is influenced by initial surface stress effects for engineering applications, where only the flexural and longitudinal modes are to be obtained. The linear size of the cross sections of the investigated nanowires models varied from 50 to 200 nm with different boundary conditions as fixed/free and fixed/fixed, where the length of the nanowire was 1000 nm.

2 Finite element formulation

2.1 3D solid element model with surface effects

Surface effects on the mechanical behavior of the nanostructures can be analyzed by adding the elements which represent the surface stresses in the finite element model. Elements derived from 4-node 2D membrane elements by introducing the zero out-of-plane coordinate were used in this research to simulate different structures of the atoms near the surface. These elements were placed on the external faces of the structure.

In order to calculate the resonant frequencies of the silicon nanowire with the surface effects taken into account, it is necessary to evaluate the stress in the whole structure which emerged due to the initial surface

stress, which is expressed as $\boldsymbol{\sigma_0} = \left\{ \sigma_{0\xi} \ \sigma_{0\eta} \ 0 \right\}^{\mathrm{T}}$ in the local coordinate system (ξ, η) of each surface element. This leads to solving the static equilibrium problem as

$$(\mathbf{K_{3D}} + \mathbf{K_s} + \mathbf{K}_{s\sigma})\,\mathbf{U} = -\mathbf{P}_s \tag{1}$$

where $\mathbf{K_{3D}}$ is the conventional structural stiffness matrix due to the solid elements without consideration of surface effects, $\mathbf{K_s}$ is the structural stiffness matrix due to the surface elements, $\mathbf{K}_{s\sigma}$ is the structural stress stiffness matrix due to the surface elements, $\mathbf{U}$ is the displacement vector, and $\mathbf{P}_s$ is the initial surface stress vector.

The stiffness matrix $\mathbf{K_{3D}}$ over the volume $\mathbf{V}$ has the form:

$$\mathbf{K_{3D}} = \int_V \mathbf{B}_{\mathbf{3D}}^{\mathbf{T}} \mathbf{D_{3D}} \mathbf{B_{3D}} dV, \tag{2}$$

where $\mathbf{B_{3D}}$ is the strain matrix of the linear 3D solid element, $\mathbf{D_{3D}}$ is the elasticity tensor.

After consideration that there is no shear stress in the surface elements, the stiffness matrix $\mathbf{K_s}$ and the stress stiffness matrix $\mathbf{K}_{s\,\sigma}$ due to surface elements over the surface $\boldsymbol{\Omega}$ are constructed, respectively, as:

$$\mathbf{K}_s = \int_{\boldsymbol{\Omega}} \mathbf{R}^{\mathbf{T}} \mathbf{B}_s^{\mathbf{T}} \mathbf{D}_s \mathbf{B}_s \mathbf{R} d\boldsymbol{\Omega}, \tag{3}$$

$$\mathbf{K}_{s\sigma} = \int_{\boldsymbol{\Omega}} \mathbf{R}^{\mathbf{T}} \left(\mathbf{N}_{\boldsymbol{\xi}}^{\mathbf{T}} \mathbf{N}_{\boldsymbol{\xi}} \sigma_{0_\xi} + \mathbf{N}_{\boldsymbol{\eta}}^{\mathbf{T}} \mathbf{N}_{\boldsymbol{\eta}} \sigma_{0_\eta} \right) \mathbf{R} d\boldsymbol{\Omega} \tag{4}$$

where $\mathbf{R}$ is the transformation matrix from local coordinates to global coordinates, $\mathbf{B}_s$ is the strain matrix of the linear membrane element in the local coordinate system matrix, and $\mathbf{D}_s$ is the elasticity tensor of the surface element. $\mathbf{N}_{\boldsymbol{\xi}}$ and $\mathbf{N}_{\boldsymbol{\eta}}$ are the derivatives of the bilinear shape function matrix $\mathbf{N}$ in the local coordinate system (ξ, η) with respect to ξ and η, respectively, where $\mathbf{N}$ is constructed of $\mathbf{N_i}$ matrices corresponding to the ith node of the element:

$$\mathbf{N_i} = \begin{bmatrix} N_i & 0 & 0 \\ 0 & N_i & 0 \end{bmatrix}. \tag{5}$$

The strain matrix $\mathbf{B}_s$ is constructed of matrix blocks $\mathbf{B_{i_s}}$, which correspond to the ith node of the element:

$$\mathbf{B_{i_s}} = \begin{bmatrix} N'_{i_\xi} & 0 & 0 \\ 0 & N'_{i_\eta} & 0 \end{bmatrix}. \tag{6}$$

Similarly, the residual surface stress vector has the form:

$$\mathbf{P}_s = \int_{\boldsymbol{\Omega}} \mathbf{R}^{\mathbf{T}} \mathbf{B}_s^{\mathbf{T}} \boldsymbol{\sigma_0} d\boldsymbol{\Omega}. \tag{7}$$

After solving the static problem, the initial stress $\boldsymbol{\sigma}^{\mathbf{i}}$ of the ith solid element can be calculated according to the obtained displacement vector:

$$\boldsymbol{\sigma}^{\mathbf{i}} = \mathbf{D}_{\mathbf{3D}}^{\mathbf{i}} \mathbf{B}_{\mathbf{3D}}^{\mathbf{i}} \mathbf{U}^{\mathbf{i}} \tag{8}$$

where $\mathbf{U}^{\mathbf{i}}$ is a displacement vector of the nodes of the ith element, $\boldsymbol{\sigma}^{\mathbf{i}} = \left\{ \sigma_x^i \ \sigma_y^i \ \sigma_z^i \ \tau_{xy}^i \ \tau_{yz}^i \ \tau_{zx}^i \right\}^{\mathrm{T}}$.

This enables to obtain the geometric stiffness matrix over the volume $\mathbf{V}$:

$$\begin{aligned} \mathbf{K}_\sigma = \int_{\mathbf{V}} \Big(& \mathbf{N}_{\mathbf{x}}^{\mathbf{T}} \mathbf{N}_{\mathbf{x}} \sigma_x + \mathbf{N}_{\mathbf{y}}^{\mathbf{T}} \mathbf{N}_{\mathbf{y}} \sigma_y + \mathbf{N}_{\mathbf{z}}^{\mathbf{T}} \mathbf{N}_{\mathbf{z}} \sigma_z + \left(\mathbf{N}_{\mathbf{x}}^{\mathbf{T}} \mathbf{N}_{\mathbf{y}} + \mathbf{N}_{\mathbf{x}}^{\mathbf{T}} \mathbf{N}_{\mathbf{y}} \right) \tau_{xy} \\ & + \left(\mathbf{N}_{\mathbf{y}}^{\mathbf{T}} \mathbf{N}_{\mathbf{z}} + \mathbf{N}_{\mathbf{z}}^{\mathbf{T}} \mathbf{N}_{\mathbf{y}} \right) \tau_{yz} + \left(\mathbf{N}_{\mathbf{z}}^{\mathbf{T}} \mathbf{N}_{\mathbf{x}} + \mathbf{N}_{\mathbf{x}}^{\mathbf{T}} \mathbf{N}_{\mathbf{z}} \right) \tau_{zx} \Big) d\mathbf{V}. \end{aligned} \tag{9}$$

Finally, the eigenvalue problem with the boundary conditions (BC) taken into consideration was solved after augmenting the stiffness matrix applied in the static problem with the geometric stiffness matrix of the solid elements:

$$\left(\mathbf{K} - \boldsymbol{\omega}^{\mathbf{2}} \mathbf{M} \right) = 0 \tag{10}$$

where $\mathbf{K} = \mathbf{K_{3D}} + \mathbf{K_s} + \mathbf{K}_{s\sigma} + \mathbf{K}_\sigma$, and $\mathbf{M}$ is the lumped mass matrix.

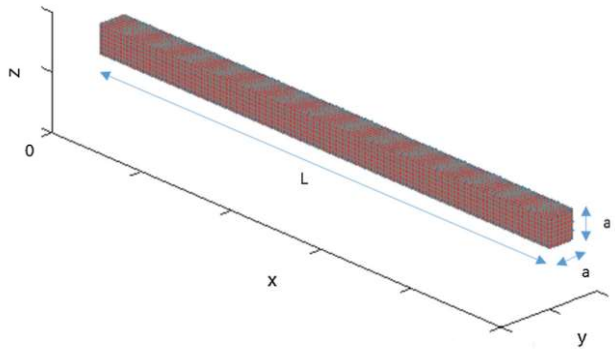

Fig. 1 The geometry of the analyzed silicon nanowire

After solving the eigenvalue problem, the equivalent Young's moduli E can be estimated if necessary. They can be approximately calculated by the formula derived according to the Euler–Bernoulli theory of flexure [26]:

$$E = \frac{4\pi^2 L^2 f_i^2 \rho A}{B_i^4 I} \tag{11}$$

where L is the length of the nanowire, f_i is the resonant frequency of the ith mode, ρ is the mass density, A is the area of the cross section, I is the geometrical moment of inertia about the neutral axis, and B_i is the constant for the ith mode based on the Euler–Bernoulli beam theory with respect to the specific BC. The values of B_i are provided in [26]. In case of the square cross section with side length a, the moment of inertia is $I = \frac{a^4}{12}$ and the cross-sectional area $A = a^2$ (Fig. 1). However, such estimations of the equivalent Young's moduli are obtained different for different cross section sizes and for different modes. Therefore, they cannot be treated as a versatile quantity for the estimation of the structural behavior at nanoscale.

2.2 2D bent beam elements model

A 2D bent beam element model can be applied as an approximation of a silicon nanowire in order to perform the flexural modal vibrations analysis. The bent beam has 3 degrees of freedom at each node $\left\{ u \; v \; v\prime \right\}^T$ corresponding to displacements in longitudinal (OX) and transverse (OY) directions together with the cross section rotation angle about OY axis. The length of the structure is L and the cross section is assumed as rectangular of the width b and height h.

In order to calculate the modal frequencies of the bent beam structure with surface effects taken into account, the initial surface stresses have to be converted into axial stresses $\boldsymbol{\sigma}_{\mathbf{0}}^{\boldsymbol{B}}$. However, the negative surface stiffness is not considered in this model. As only the stresses of the top and the bottom surfaces of the models are taken into account in the 2D bent beam model, the initial stresses $\boldsymbol{\sigma}_{\mathbf{0}}$ were recalculated using formula:

$$\boldsymbol{\sigma}_{\mathbf{0}}^{\boldsymbol{B}} = \frac{2\boldsymbol{\sigma}_{\mathbf{0}}}{h}. \tag{12}$$

This leads to solving static equilibrium problem as

$$\left(\mathbf{K}_{\mathbf{0}}^{\boldsymbol{B}} + \mathbf{K}_{\boldsymbol{\sigma}}^{\boldsymbol{B}}\right)\mathbf{U} = -\mathbf{P}^{\mathbf{B}} \tag{13}$$

where $\mathbf{K}_{\mathbf{0}}^{\boldsymbol{B}}$ is the stiffness matrix of the bent beam element and $\mathbf{K}_{\boldsymbol{\sigma}}^{\boldsymbol{B}}$ is the stress stiffness matrix, $\mathbf{U}$ is the displacement vector, and $\mathbf{P}^{\mathbf{B}}$ is the vector of the forces emerged due to the initial stresses.

The stiffness matrix $\mathbf{K}_{\mathbf{0}}^{\boldsymbol{B}}$ over the length L of the structure has the form:

$$\mathbf{K}_{\mathbf{0}}^{\boldsymbol{B}} = Eb \int_{\mathbf{0}}^{\boldsymbol{L}} \int_{-h/2}^{h/2} \mathbf{B}^{\mathbf{T}}\mathbf{B}\mathrm{d}y\mathrm{d}x \tag{14}$$

where E is Young's modulus, and $\mathbf{B}$ is the strain matrix of the bent beam element:

$$\mathbf{B} = \left[\frac{\partial}{\partial x} \; -y\frac{\partial^2}{\partial x^2} \right] \mathbf{N} \tag{15}$$

where $\mathbf{N}$ is the shape functions matrix of the bent beam element.

The stress stiffness matrix $\mathbf{K}_{\sigma}^{B}$ is constructed over the length L of the structure as:

$$\mathbf{K}_{\sigma}^{B} = b \int_{\mathbf{0}}^{L} \int_{-\frac{h}{2}}^{\frac{h}{2}} \mathbf{N}_{\mathbf{x}}'^{\mathbf{T}} \mathbf{N}_{\mathbf{x}}' \boldsymbol{\sigma}_{\mathbf{0}}^{B} \mathrm{d}y\mathrm{d}x. \tag{16}$$

The loading force vector due to initial surface stress reads:

$$\mathbf{P}^{\mathbf{B}} = b \int_{\mathbf{0}}^{L} \int_{-h/2}^{h/2} \mathbf{B}^{\mathbf{T}} \boldsymbol{\sigma}_{\mathbf{0}}^{B} \mathrm{d}y\mathrm{d}x. \tag{17}$$

After solving the static equilibrium problem matrix, $\mathbf{K}_{\sigma}^{F}$ is constructed for the structure with the obtained displacements, and the eigenvalue problem is solved by taking into account the appropriate boundary conditions at the ends of the beam:

$$\left(\mathbf{K} - \boldsymbol{\omega}^2 \mathbf{M}\right) = 0 \tag{18}$$

where $\mathbf{K} = \mathbf{K}_{\mathbf{0}}^{B} + \mathbf{K}_{\sigma}^{B}$, and $\mathbf{M}$ is the mass matrix:

$$\mathbf{M} = b\rho \int_{\mathbf{0}}^{L} \int_{-h/2}^{h/2} \mathbf{N}^{\mathbf{T}} \mathbf{N} \mathrm{d}y\mathrm{d}x \tag{19}$$

where ρ is the mass density of the material.

3 Numerical experiments

The numerical experiments were performed in order to investigate the influence of the surface effects on the modal frequencies of the nanostructure. The resonant frequencies were calculated by solving the linear eigenvalue problem in Eq. (10). The modal frequencies obtained for the model with surface effects taken into consideration were compared with the modal frequencies obtained for the model without surface stress effects taken into account. Moreover, the natural frequencies for the flexural and longitudinal modes were calculated using the 2D bent beam model and were compared in a similar manner with the beam model without surface stress effects.

The geometry of the structure was a rectangular parallelepiped with square cross section, which can be considered as an approximation of a nanowire. The length of the structure in X direction was 1000 nm. Length a of the cross section side was varied from 50 to 200 nm. This set of cross section side length values enables to observe the increasing influence of surface stresses on the modal frequencies as the cross section area decreases. The influence of surface stresses in the FE model is expressed via the stress stiffness matrix component in Eq. (1), which modifies the effective stiffness of the structure. Figure 2 displays the distribution

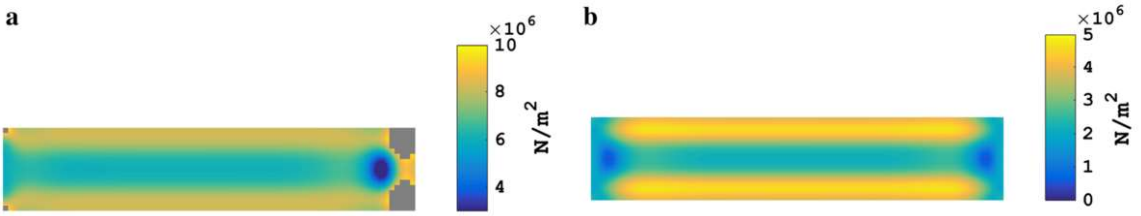

Fig. 2 Equivalent von Mises stress distribution over the volume of the nanowire ($a = 200$ nm) for the fixed/free (**a**) and fixed/fixed boundary conditions (**b**)

of initial equivalent von Mises stresses over the volume of the body due to the action of surface stresses, where $a = 200$ nm. The gray areas in Fig. 2 represent the regions where the stress value exceeds the maximum values of the color scale selected for representing stresses in this Figure. Otherwise, the representation of stress concentration areas at the corners of the structure by a color would mask the visibility of the distribution of modest stress values over the remaining volume of the structure.

Two cases of BC as fixed/free and fixed/fixed at the ends of the structure were analyzed in the numerical examples. For the fixed/free BC, the nodal displacements at the left-hand side of the model $(-x)$ were fully constrained. For the fixed/fixed BC, the nodal displacements were fully constrained at both the left $(-x)$ and right-hand side $(+x)$ surfaces. The regular mesh of 3D solid hexahedral elements was used for the models in all numerical simulations.

The material parameters used in the numerical simulations were consistent with the material parameters given in [20]: mass density $2.33\,\mathrm{g\,cm^{-3}}$, the elastic constants of silicon are $C_{11} = 161.66$ GPa, $C_{12} = 81.599$ GPa, $C_{44} = 60.274$ GPa, and the elastic constants of silicon surface are $S_{11} = -10.64\,\mathrm{N\,m^{-1}}$, $S_{12} = -3.88\,\mathrm{N\,m^{-1}}$, the initial surface stress $\sigma_0 = 0.6\,\mathrm{N\,m^{-1}}$.

For the bent beam element, Young's modulus equal to $E = 107$ GPa was used. This value was calculated based on C_{11} and C_{12} values with the assumption that Poisson's ratio $\nu = 0.3354$ was applied. The initial surface stress was recalculated to axial stress with respect to the geometry of each structure.

The analysis was performed for the first three flexural, torsional, and longitudinal modes of the structure.

The first three flexural vibration (V) modes of the structure are shown in Fig. 3. As the cross section of the structure is square, vibrational modes of uniform beams exist in pairs representing the same behavior in the two perpendicular planes. The modal frequencies were employed to calculate the equivalent Young's modulus according to the Euler–Bernoulli beam theory. For the fixed/free BC, the constants B_i [see Eq. (11)] are equal to $B_1 = 1.875$, $B_2 = 4.694$, $B_3 = 7.855$ for the first, second, and third flexural modes, respectively. For the fixed/fixed BC, the values $B_1 = 4.730$, $B_2 = 7.853$, $B_3 = 10.996$ were used to calculate equivalent Young's moduli [26].

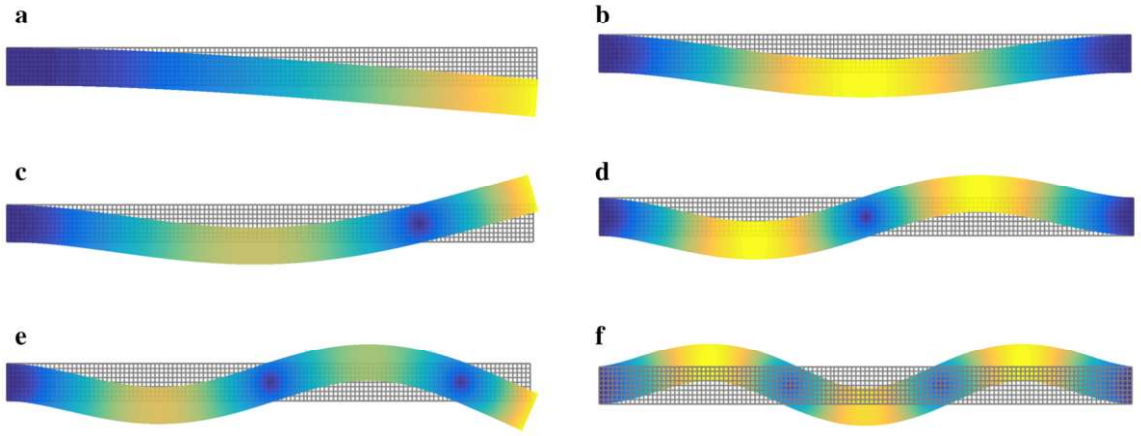

Fig. 3 The shape of the flexural vibrational modes for the fixed/free (**a**, **c**, **e**) and fixed/fixed (**b**, **d**, **f**) boundary conditions

Table 1 Equivalent Young's moduli calculated using flexural modes

Width a (nm)	Equivalent Young's moduli ($\mathrm{N\,m^{-2}}$)					
	Fixed/free BC			Fixed/fixed BC		
	1st V mode	2nd V mode	3rd V mode	1st V mode	2nd V mode	3rd V mode
200	1.0537E+11	8.3182E+10	6.3267E+10	8.2688E+10	6.0383E+10	4.5010E+10
150	1.0553E+11	9.2464E+10	7.6947E+10	9.2718E+10	7.4971E+10	6.0135E+10
100	1.0204E+11	9.9794E+10	9.1209E+10	1.0141E+11	9.0731E+10	7.9701E+10
90	9.9716E+10	1.0053E+11	9.3638E+10	1.0263E+11	9.3527E+10	8.3738E+10
80	9.6334E+10	1.0111E+11	9.6020E+10	1.0394E+11	9.6371E+10	8.7915E+10
70	9.0555E+10	1.0104E+11	9.7989E+10	1.0502E+11	9.8911E+10	9.1873E+10
60	8.0259E+10	1.0008E+11	9.9516E+10	1.0605E+11	1.0126E+11	9.5652E+10
50	5.9568E+10	9.7149E+10	1.0016E+11	1.0700E+11	1.0331E+11	9.9051E+10

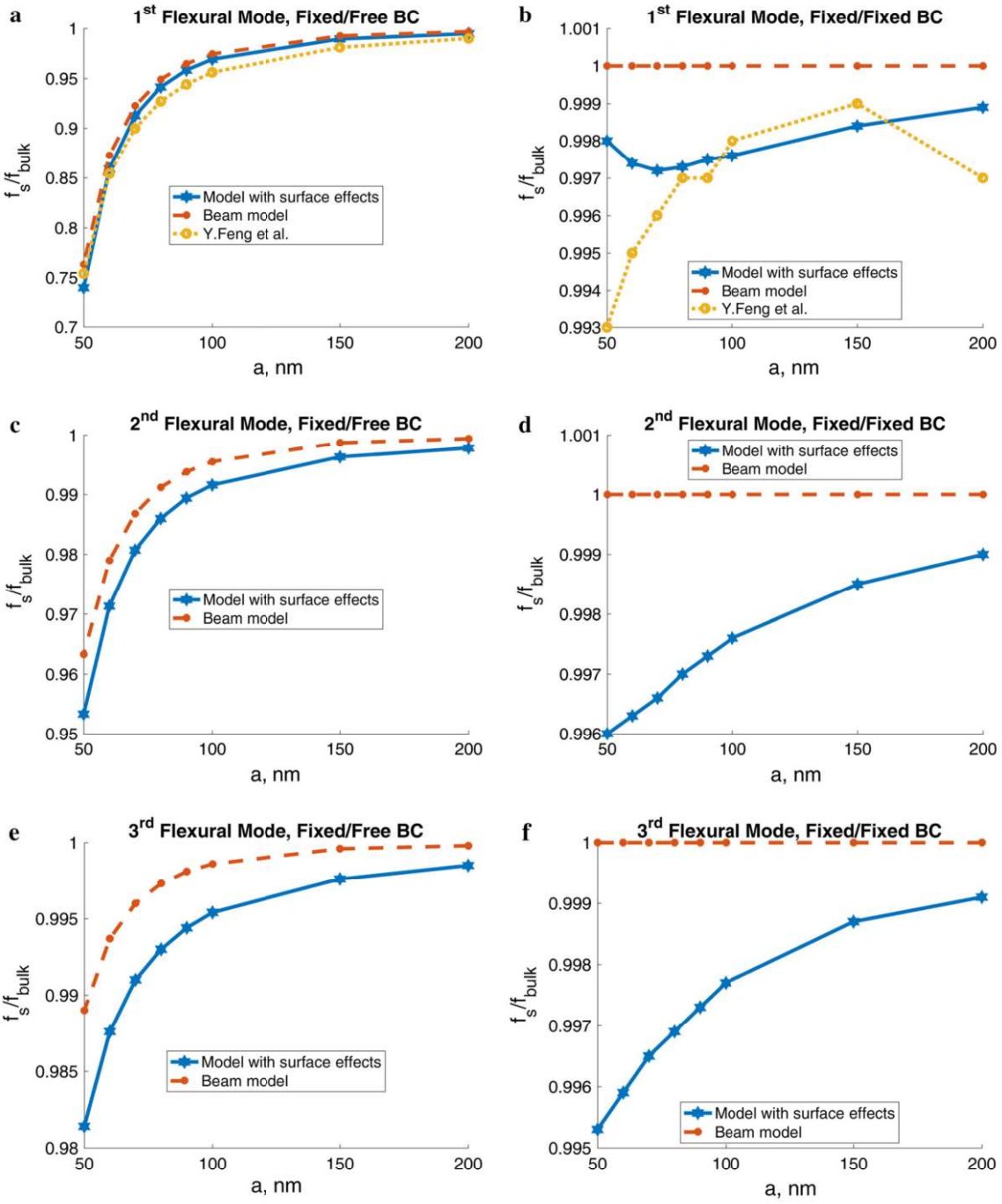

Fig. 4 The ratios of the frequencies of the vibrational modes for the fixed/free (**a**, **c**, **e**) and fixed/fixed (**b**, **d**, **f**) boundary conditions

The equivalent Young's moduli (EYM) which were calculated for each vibration mode of structures with various geometry are provided in Table 1. The EYM values obtained for each mode differ significantly due to several reasons. Firstly, the Euler–Bernoulli beam theory is maintained for the thin beams only as the shear effects are neglected. This causes the differences of more than 10% between the EYM obtained for the different modes under both BCs for the structures with the length-to-width ratio less than 10 ($a = 200$ nm, $a = 150$ nm). Such structures should be considered as thick beams. Secondly, the surface effects have significant influence for the structures with the small width ($a < 70$ nm) under the fixed/free BC as the surface area-to-volume ratio is larger as compared to other structures.

The results clearly demonstrate that the values of the equivalent Young's moduli are dependent on the size of the cross section, as well as on the type and number of the mode. Therefore, EYM values could be considered only as an approximation for taking into account the reduction of the effective stiffness of nanostructures. Obviously, usage of equivalent Young's modulus is hardly possible when poly-harmonic vibrations are analyzed.

The influence of the surface effects was analyzed by means of the ratio calculated as the frequency obtained for the structure with surface effects taken into account and the frequency obtained for the structure of the bulk elements. Moreover, the results (ratios) were compared with the ratios calculated for the frequencies obtained for the 2D bent beam structure with and without initial stress taken into account.

The ratios of the frequencies obtained for the first three flexural modes under fixed/free and fixed/fixed BC for the considered structures with various values of the width of cross sections are shown in Fig. 4. The ratios of the first flexural mode were compared with the corresponding ratios provided in [20], where they were obtained relying on the bulk model with the two-dimensional elements which represent surface properties. For the fixed/free BC, the difference between the ratios of frequencies for the structures with and without the surface elements obtained in this research and by [20] did not exceed 3% for the respective structures. Similarly, for the fixed/fixed BC, the difference did not exceed 2%.

For the first flexural mode under the fixed/free BC, the ratios obtained for the 2D bent beam model agree with the ratio for the solid element model with surface effects taken into account as the difference between the values does not exceed 2% for all geometries. However, the surface effects for the structure under the fixed/free BC have a small influence on the values of the second and third flexural modes as the ratios for the 3D model with the surface effects taken into account are close to 1.

For the flexural modes of the structure under the fixed/fixed BC, the ratio of the flexural frequencies obtained for the structures with and without surface effects taken into account is approximately equal to 1 for all analyzed structures. The ratios calculated for the beam model are not influenced by the initial stresses at all. This tendency in both models occurs due to the boundary conditions as the constraints in both ends result in the same configuration of the structure in the initial state and after solving the static equilibrium problem [11].

It should be noted that the frequencies obtained for the 3D model and beam model without surface effects taken into account differ significantly for the second and third flexural modes. This is caused by the fact that the beam model is based on the Euler–Bernoulli flexure theory which holds for the thin structures as long as shear has an insignificant impact on the result. As the width of the cross section increases, the shear effects have more significant impact on the vibrational frequencies, and this results in significant differences of the calculated ratios. However, the influence of the initial surface stress evaluated as a ratio of the frequencies, obtained for the respective model with and without surface effects shows good agreement for both solid elements and beam models.

The torsional modes under the fixed/free and fixed/fixed BCs are shown in Fig. 5.

The ratios of frequencies of torsional modes are given in Fig. 6. In case the surface effects are considered, the frequencies are significantly lower for structures with smaller cross sections for both fixed/free and fixed/fixed BCs. The shear terms were not included in the analyzed 2D bent beam model; therefore, it was not possible to obtain the frequency value for the torsional mode.

The longitudinal modes under the fixed/free and fixed/fixed BCs are shown in Fig. 7.

For the longitudinal modes, the ratios of the frequencies with and without surface effects considered are approximately equal to 1 for all the analyzed structures and both fixed/free and fixed/fixed BCs (Fig. 8). This indicates that the surface effects are insignificant for the longitudinal mode. The ratios obtained for the bent beam model agree with the results obtained for the solid element model with the ratios equal to 1 for both types of BCs.

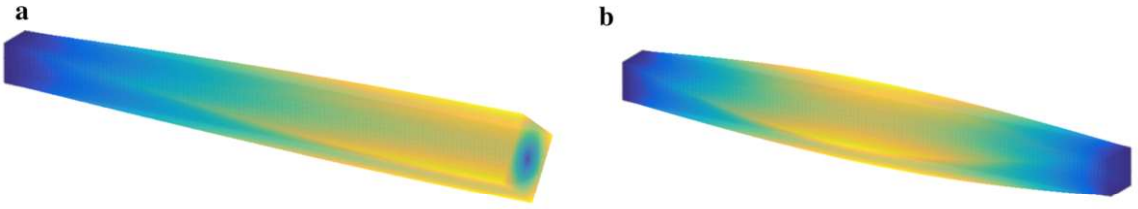

Fig. 5 The shape of the torsional modes for the fixed/free (**a**) and fixed/fixed (**b**) boundary conditions

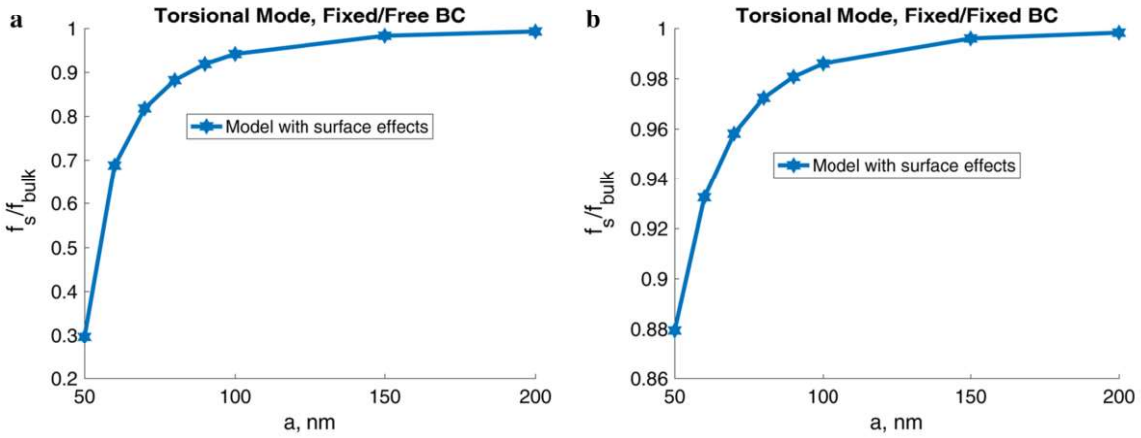

Fig. 6 The ratios of the frequencies of the torsional mode for the fixed/free (**a**) and fixed/fixed (**b**) boundary conditions

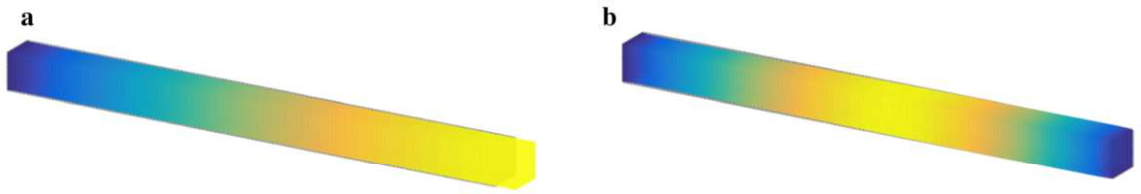

Fig. 7 The shape of the frequencies of the longitudinal modes for the fixed/free (**a**) and fixed/fixed (**b**) boundary conditions

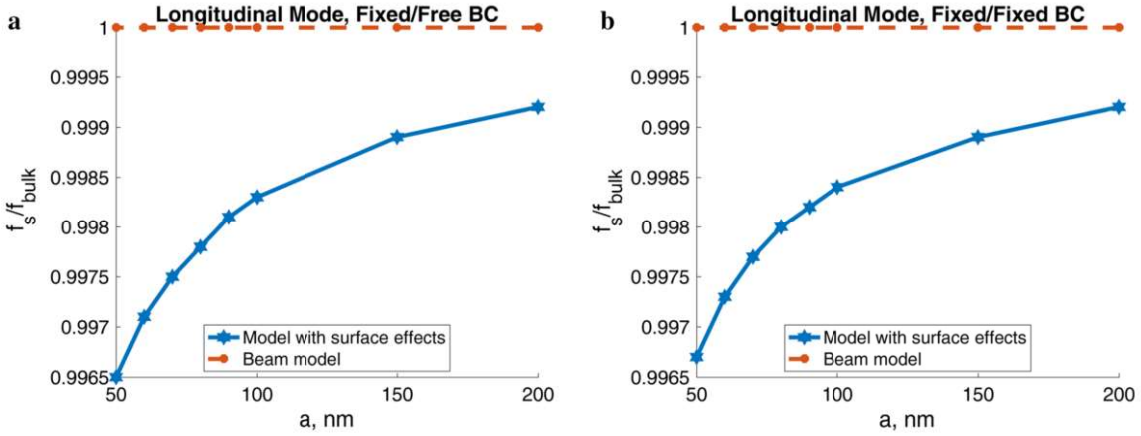

Fig. 8 The ratios of the longitudinal mode for the fixed/free (**a**) and fixed/fixed (**b**) boundary conditions

4 Conclusions

For the nanostructures, the initial surface stress effects cannot be neglected in calculations. Up to now, many authors addressed this problem, and different approaches have been proposed. They were meant to take into account the smaller structural stiffness and therefore smaller modal frequencies exhibited at the nanoscale compared to the corresponding quantities calculated by the conventional macroscale-type models. Appropriate corrections of the Young's moduli up to certain equivalent values and addition of surface element layers of certain negative stiffness enable to obtain the results which match the experimental observations.

It was demonstrated that the surface effects can be neglected if the structure is considered thick as the ratios of frequencies with and without surface effects taken into account are close to 1 if the length-to-width ratio is less than 10. However, they are significant for the thin structures under the fixed/free boundary conditions. In contrast to the fixed/free boundary conditions, the surface effects do not influence the flexural frequencies of the structure under the fixed/fixed boundary conditions. Although the surface effects are significant in the

torsional modes, they are insignificant in longitudinal mode under both fixed/free and fixed/fixed boundary conditions.

The equivalent Young's moduli calculated using frequencies obtained for the model with surface effects taken into account should be used in the later analysis carefully since the values obtained for different modes and boundary conditions differ significantly.

The ratios were compared with the ratios calculated for the 2D bent beam structure. It has been shown that the beam model is a good approximation of the nanowires with the small cross-sectional area in vibrational analysis. However, in order to obtain the values of the torsional modes, the more advanced beam models should be applied.

Acknowledgements This research was supported by the Research, Development and Innovation Fund of Kaunas University of Technology (FEMSHORTWAVE. PP32/1808).

References

1. Shamloo, A., Mehrafrooz, B.: Nanomechanics of actin filament: a molecular dynamics simulation. Cytoskeleton **75**, 118–130 (2018). https://doi.org/10.1002/cm.21429
2. Sinnott, S.B., Heo, S.-J., Brenner, D.W., Harrison, J.A., Irving, D.L.: Computer simulations of nanometer-scale indentation and friction. In: Nanotribology and Nanomechanics, pp. 301–370. Springer, Cham (2017). https://doi.org/10.1007/978-3-319-51433-8_7
3. Duan, H.L., Wang, J., Karihaloo, B.L.: Theory of Elasticity at the Nanoscale. Elsevier Masson SAS, Amsterdam (2009). https://doi.org/10.1016/S0065-2156(08)00001-X
4. Craighead, H.G.: Nanoelectromechanical systems. Science **290**, 1532–1535 (2000). https://doi.org/10.1126/science.290.5496.1532
5. Abazari, A.M., Safavi, S.M., Rezazadeh, G., Villanueva, L.G.: Modelling the size effects on the mechanical properties of micro/nano structures. Sensors (Switzerland) **15**, 28543–28562 (2015). https://doi.org/10.3390/s151128543
6. Feng, X.L., He, R., Yang, P., Roukes, M.L.: Very high frequency silicon nanowire electromechanical resonators. Nano Lett. **7**, 1953–1959 (2007). https://doi.org/10.1021/nl0706695
7. Pishkenari, H.N., Afsharmanesh, B., Tajaddodianfar, F.: Continuum models calibrated with atomistic simulations for the transverse vibrations of silicon nanowires. Int. J. Eng. Sci. **100**, 8–24 (2016). https://doi.org/10.1016/j.ijengsci.2015.11.005
8. Yu, H., Sun, C., Zhang, W.W., Lei, S.Y., Huang, Q.A.: Study on size-dependent Young's modulus of a silicon nanobeam by molecular dynamics simulation. J. Nanomater. (2013). https://doi.org/10.1155/2013/319302
9. Wu, J.X., Li, X.F., Tang, A.Y., Lee, K.Y.: Free and forced transverse vibration of nanowires with surface effects. JVC/J. Vib. Control **23**, 2064–2077 (2017). https://doi.org/10.1177/1077546315610302
10. Ansari, R., Sahmani, S.: Bending behavior and buckling of nanobeams including surface stress effects corresponding to different beam theories. Int. J. Eng. Sci. **49**, 1244–1255 (2011). https://doi.org/10.1016/j.ijengsci.2011.01.007
11. Song, F., Huang, G.L., Park, H.S., Liu, X.N.: A continuum model for the mechanical behavior of nanowires including surface and surface-induced initial stresses. Int. J. Solids Struct. **48**, 2154–2163 (2011). https://doi.org/10.1016/j.ijsolstr.2011.03.021
12. Jiang, L.Y., Yan, Z.: Timoshenko beam model for static bending of nanowires with surface effects. Phys. E Low-Dimens. Syst. Nanostruct. **42**, 2274–2279 (2010). https://doi.org/10.1016/j.physe.2010.05.007
13. Park, H.S., Klein, P.A.: A surface Cauchy–Born model for silicon nanostructures. Comput. Methods Appl. Mech. Eng. **197**, 3249–3260 (2008). https://doi.org/10.1016/j.cma.2007.12.004
14. Nasr Esfahani, M., Yilmaz, M., Sonne, M.R., Hattel, J.H., Alaca, B.E.: Selecting the optimum engineering model for the frequency response of FCC nanowire resonators. Appl. Math. Model **44**, 236–245 (2017). https://doi.org/10.1016/j.apm.2016.10.022
15. Nasr Esfahani, M., Alaca, B.E.: Surface stress effect on silicon nanowire mechanical behavior? Size Orient. Depend. **127**, 112–123 (2018)
16. Eltaher, M.A., Khater, M.E., Emam, S.A.: A review on nonlocal elastic models for bending, buckling, vibrations, and wave propagation of nanoscale beams. Appl. Math. Model. **40**, 4109–4128 (2016). https://doi.org/10.1016/j.apm.2015.11.026
17. Park, H.S.: Surface stress effects on the resonant properties of silicon nanowires. J. Appl. Phys. **103**, 123504 (2008). https://doi.org/10.1063/1.2939576
18. Wang, Z.Q., Zhao, Y.P., Huang, Z.P.: The effects of surface tension on the elastic properties of nano structures. Int. J. Eng. Sci. **48**, 140–150 (2010). https://doi.org/10.1016/j.ijengsci.2009.07.007
19. Wang, G.F., Feng, X.Q.: Effects of surface elasticity and residual surface tension on the natural frequency of microbeams. Appl. Phys. Lett. **90**, 1–4 (2007). https://doi.org/10.1063/1.2746950
20. Feng, Y., Liu, Y., Wang, B.: Finite element analysis of resonant properties of silicon nanowires with consideration of surface effects. Acta Mech. **217**, 149–155 (2011). https://doi.org/10.1007/s00707-010-0388-4
21. Cuenot, S., Frétigny, C., Demoustier-Champagne, S., Nysten, B.: Surface tension effect on the mechanical properties of nanomaterials measured by atomic force microscopy. Phys. Rev. B. **69**, 165410 (2004). https://doi.org/10.1103/PhysRevB.69.165410
22. Wang, G., Li, X.: Size dependency of the elastic modulus of ZnO nanowires: surface stress effect. Appl. Phys. Lett. **91**, 231912 (2007). https://doi.org/10.1063/1.2821118
23. Lee, B., Rudd, R.E.: First-principles study of the Young's modulus of Si <001> nanowires. Phys. Rev. B. **75**, 041305 (2007). https://doi.org/10.1103/PhysRevB.75.041305

24. Fan, T., Yang, L.: Effective Young's modulus of nanoporous materials with cuboid unit cells. Acta Mech. **228**, 21–29 (2017). https://doi.org/10.1007/s00707-016-1682-6
25. Zhu, Y., Xu, F., Qin, Q., Fung, W.Y., Lu, W.: Mechanical properties of vapor–liquid–solid synthesized silicon nanowires. Nano Lett. **9**, 3934–3939 (2009). https://doi.org/10.1021/nl902132w
26. Stokey, W.F.: Vibration of systems having distributed mass and elasticity. In: Harris, C.M., Piersoll, A. (eds.) Shock and Vibration Handbook, Chap. 7. McGraw-Hill, New York (2002)

Publisher's Note Springer Nature remains neutral with regard to jurisdictional claims in published maps and institutional affiliations.